

Cite this article as: Li Yong, Yan Feng, Zhang Jing, et al. Mechanical Constitutive Model for Equivalent Solid of Fission Gas Bubbles in Irradiated U-10Mo Fuels[J]. Rare Metal Materials and Engineering, 2025, 54(07): 1653-1660. DOI: <https://doi.org/10.12442/j.issn.1002-185X.20240640>.

ARTICLE

Mechanical Constitutive Model for Equivalent Solid of Fission Gas Bubbles in Irradiated U-10Mo Fuels

Li Yong^{1,2}, Yan Feng², Zhang Jing², Zang Liye¹, Ding Shurong²

¹China Nuclear Power Technology Research Institute Co., Ltd, Shenzhen 518026, China; ²Institute of Mechanics and Computational Engineering, Department of Aeronautics and Astronautics, Fudan University, Shanghai 200433, China

Abstract: The internal pressure within fission gas bubbles (FGBs) in irradiated nuclear fuels drives mechanical interactions with the surrounding fuel skeleton. To investigate the micromechanical stress fields in irradiated nuclear fuels containing pressurized FGBs, a mechanical constitutive model for the equivalent solid of FGBs was developed and validated. This model was based on the modified Van der Waals equation, incorporating the effects of surface tension. Using this model, the micromechanical fields in irradiated U-10Mo fuels with randomly distributed FGBs were calculated during uniaxial tensile testing via the finite element (FE) method. The macroscopic elastic constants of the irradiated U-10Mo fuels were then derived using homogenization theory, and the influences of bubble pressure, bubble size, and porosity on these constants were examined. Results show that adjacent FGBs exhibit mechanical interactions, which leads to distinct stress concentrations in the surrounding fuel skeleton. The macroscopic elastic constants of irradiated U-10Mo fuels decrease with increasing the macroscopic porosity, which can be quantitatively described by the Mori-Tanaka model. In contrast, bubble pressure and size have negligible effects on these constants.

Key words: effective mechanical constitutive model; fission gas bubbles; FE method; U-10Mo nuclear fuels; macroscopic elastic constants

1 Introduction

During irradiation in reactors, both solid and gaseous products are generated in nuclear fuels through the fission process. Among these products, fission gases are of particular concern due to their significant impact on fuel performance. They induce changes in the microstructure, physical properties, stress fields, and swelling deformation of nuclear fuels^[1-6]. On average, one fission gas atom (xenon or krypton) is produced for every four fission events^[7-8]. These fission gas atoms tend to form fission gas bubbles (FGBs) due to their low solubility in the nuclear fuel matrix^[9]. Transmission electron microscopy (TEM) and scanning electron microscopy (SEM) studies have revealed that FGBs are distributed both within the grains (intragranular) and along the grain boundaries (intergranular) of the nuclear fuel^[10-11]. Meanwhile, the density of intergranular bubbles increases with burnup, and

micrometer-sized FGBs are randomly distributed throughout the grains in high-burnup fuels^[12].

The formation and growth of FGBs transform irradiated nuclear fuels into porous structures, thereby degrading their macroscopic thermal conductivity and elastic modulus. The evolution of these macroscopic properties can be described as functions of the macroscopic porosity of the irradiated fuels^[2-3,9,13]. As FGBs become filled with fission gas atoms, internal bubble pressure develops within the bubbles. In irradiated U-Mo fuels, this bubble pressure ranges from several MPa to hundreds of MPa^[14]. The pressure is determined by the temperature, volume of FGBs, and the number of fission gas atoms, as described by the modified Van der Waals equation^[15-18]. These pressurized FGBs mechanically interact with the surrounding solid fuel matrix and are also constrained by the surface tension of the bubbles^[3-4].

In models of fission gas swelling, bubble pressure is

Received date: September 30, 2024

Foundation item: National Natural Science Foundation of China (12135008, 12132005)

Corresponding author: Ding Shurong, Ph. D., Professor, Institute of Mechanics and Computational Engineering, Department of Aeronautics and Astronautics, Fudan University, Shanghai 200433, P. R. China, Email: dingshurong@fudan.edu.cn; Zhang Jing, Ph. D., Institute of Mechanics and Computational Engineering, Department of Aeronautics and Astronautics, Fudan University, Shanghai 200433, P. R. China, Email: jj_zhang@fudan.edu.cn

Copyright © 2025, Northwest Institute for Nonferrous Metal Research. Published by Science Press. All rights reserved.

typically expressed as the sum of surface tension and the macroscale hydrostatic pressure of the homogenized porous fuels^[17-18]. However, the equivalent spherical shell model^[18], which is based on a single bubble, cannot precisely capture the complex mechanical fields in irradiated fuels with numerous FGBs, although it can be used to estimate macroscale swelling strains. To address this restriction, Cao et al^[4] developed a pore pressure model for FGBs in UO₂ fuels, considering pore size characteristics and burnup conditions. They established a 2D finite element (FE) model of the fuel particle with non-uniformly distributed FGBs to calculate the stress fields in high-burnup UO₂ fuels. In their studies, bubble pressure was applied as a load boundary condition on the bubble surfaces within the UO₂ particle. However, this applied pressure remained constant and did not vary with the deformation of the fuel skeleton or FGBs. To better reflect the relationship between bubble pressure and the deformation of FGBs, it is necessary to develop an effective mechanical constitutive model for FGBs. Jiang et al^[19] proposed a method for 3D simulation of internal gas effects on thermal-mechanical behavior in nuclear fuel elements. In their approach, the internal gas volume was represented by an equivalent solid with a constant elastic modulus. However, this model does not satisfy the modified Van der Waals equation, which describes the relationship between the variation in pressure and the internal gas volume.

In this study, a mechanical constitutive model for the equivalent solid of FGBs is derived based on the modified Van der Waals equation, incorporating the effect of surface tension. Using this model, the mechanical response of FGBs and the interaction between FGBs and the surrounding fuel skeleton under varying external loads are calculated. FE simulations of uniaxial tensile tests are performed on irradiated U-10Mo fuels containing pressurized FGBs. The macroscopic elastic constants of these fuels are then determined using homogenization theory, based on the microscopic mechanical fields within FGBs and the U-10Mo fuel skeleton. The effects of bubble pressure, bubble size, and porosity on the macroscopic elastic constants were investigated. Additionally, the calculated macroscopic elastic constants were compared with the experimental data in reference and results from other theoretical models to validate the applicability of the proposed mechanical constitutive model for FGBs.

2 Effective Mechanical Constitutive Model for FGBs

Spherical models are generally used to describe the geometry of FGBs^[4,6,18,20]. The force analysis for a spherical FGB is shown in Fig. 1. The constraint pressure of the surrounding fuel skeleton, bubble pressure, and surface tension satisfy the force balance equation, as follows:

$$P_b = P_s + \frac{2\gamma}{R} \quad (1)$$

where P_b is the current bubble pressure; γ is the surface tension of FGB; R is the bubble radius; P_s is the constraint pressure exerted by the surrounding fuel skeleton, also termed

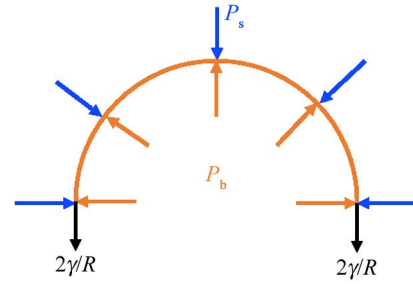


Fig.1 Force analysis of FGB

as the effective hydrostatic pressure of FGB in this study. P_s is the actual pressure subjected to the surrounding fuel skeleton.

According to the modified Van der Waals equation^[5,17], the bubble pressure is determined by the temperature, the number of fission gas atoms, and the volume of FGB, as follows:

$$P_b(V - h_s b_v N) = NkT \quad (2)$$

where V is the bubble volume with $V = 4\pi R^3/3$; N is the number of fission gas atoms in the fission gas bubble; k is the Boltzmann constant; b_v is the Van der Waals constant for Xe gas; h_s is the fitting parameter according to the hard sphere model.

In this study, a FGB is modeled as an equivalent solid with the goal of developing an effective mechanical constitutive equation that describes the mechanical interactions between FGBs and the surrounding fuel matrix. For given values of temperature and the number of fission gas atoms, it is necessary to establish the relationship between the volume change and the bubble pressure variation. According to the modified Van der Waals equation, the ratio of the current bubble volume V to the initial bubble volume V_0 can be expressed as follows:

$$\frac{V}{V_0} = \frac{NkT/P_b + h_s b_v N}{N_0 k T_0 / P_{b0} + h_s b_v N_0} \quad (3)$$

where P_{b0} , N_0 , and T_0 denote the initial bubble pressure, the number of fission gas atoms, and the temperature before the volume changes, respectively.

The volume ratio can also be expressed as a function of the volumetric strain, as follows:

$$\frac{V}{V_0} = e^{\varepsilon_{ik}} \quad (4)$$

where ε_{ik} depicts the first invariant of the logarithmic strain tensor, which refers to the volumetric strain relative to the reference configuration.

Combining Eq. (3) and Eq. (4), the current bubble pressure can be obtained, as follows:

$$\begin{aligned} P_b &= \frac{NkT}{e^{\varepsilon_{ik}}(N_0 k T_0 / P_{b0} + N_0 h_s b_v) - h_s b_v N} \\ &= \frac{c_1}{e^{\varepsilon_{ik}} c_2 - c_3} \end{aligned} \quad (5)$$

where $c_1 = NkT$; $c_2 = N_0 k T_0 / P_{b0} + N_0 h_s b_v$; $c_3 = h_s b_v N$.

According to Eq. (1) and Eq. (5), the effective hydrostatic pressure of FGB is expressed as follows:

$$P_s = \frac{c_1}{e^{\epsilon_{ik}} c_2 - c_3} - \frac{2\gamma}{R_0 e^{\frac{1}{3}\epsilon_{ik}}} \quad (6)$$

where R_0 represents the initial radius of FGB.

Thus, the effective mechanical constitutive equation for the equivalent solid of FGB is developed as follows:

$$\sigma_{ij} = -P_s \delta_{ij} = \left(-\frac{c_1}{e^{\epsilon_{ik}} c_2 - c_3} + \frac{2\gamma}{R_0 e^{\frac{1}{3}\epsilon_{ik}}} \right) \delta_{ij} \quad (7)$$

where σ_{ij} denotes the stress components; δ_{ij} represents the Kronecker delta. For a given time increment, the stresses at the end can be calculated using the initial configuration as the reference one. Herein, the volumetric strain represents the incremental strain relative to the initial state.

To compute the mechanical response of the equivalent solid for FGBs using FE method, the consistent stiffness modulus

$D_{ijkl} = \frac{\partial \sigma_{ij}}{\partial \epsilon_{kl}}$ is needed for the equilibrium iteration. According

to Eq. (7), the corresponding consistent stiffness modulus can be derived as follows:

$$D_{ijkl}^s = \left[\frac{c_1 c_2 e^{\epsilon_{mm}}}{(e^{\epsilon_{mm}} c_2 - c_3)^2} - \frac{2\gamma e^{\frac{1}{3}\epsilon_{mm}}}{3R_0 e^{\frac{2}{3}\epsilon_{mm}}} \right] \delta_{ij} \delta_{kl} \quad (8)$$

where D_{ijkl} denotes the consistent stiffness modulus, ϵ_{mm} represents the first invariant of the logarithmic strain tensor, and δ_{kl} is the Kronecker delta.

3 Verification of Effective Mechanical Constitutive Equation for Equivalent Solid of FGBs

The mechanical constitutive equation for the equivalent solid of FGBs, derived based on the modified Van der Waals equation and the effect of surface tension, provides a foundation for numerically calculating the thermomechanical behavior of porous nuclear fuels. To validate the established constitutive equation, a spherical model containing FGB and the U-10Mo fuel skeleton was constructed to simulate the mechanical response under the external pressure. Given the geometric and loading symmetry, 1/8 of the spherical model was selected as FE model, as shown in Fig.2. The model was discretized into 96 876 elements using the C3D8R element type. Symmetric boundary conditions were applied to the surfaces at $x=0$, $y=0$, and $z=0$, which corresponded to the symmetric planes of the 1/8 spherical model. An external pressure is applied to the outer surface of the model. Based on Ref. [14], the initial bubble pressure and bubble radius were set as 50 MPa and 0.2 μm , respectively. The volume fraction of FGB (f_v) is set as 10%. The temperature and the number of fission gas atoms in FE model were assumed to remain constant during the application of the external pressure. FE simulation was performed using the commercial software ABAQUS with the mechanical constitutive equation for the equivalent solid of FGBs implemented via a user-defined subroutine UMAT.

The hydrostatic pressure results of FE model with the pressured FGB are shown in Fig.3. The effective hydrostatic

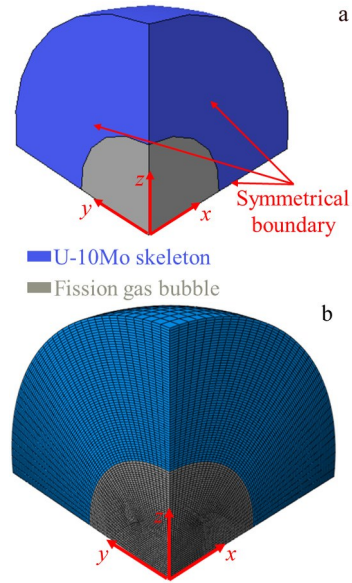


Fig.2 Schematic diagram (a) and mesh grid (b) of FE model containing equivalent solid of FGB and U-10Mo skeleton

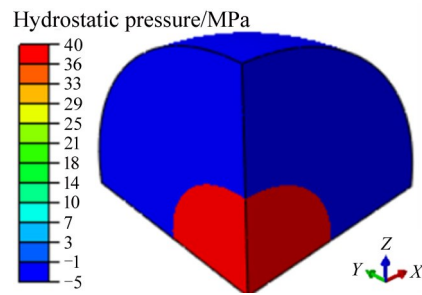


Fig.3 Contour plot of hydrostatic pressure in FE model with pressured FGB before applying external pressure

pressure of FGB is approximately 40 MPa, which is lower than the initial bubble pressure of 50 MPa. This difference is attributed to the constraint effect of surface tension on FGB. For a FGB with radius of 0.2 μm , the equivalent constraint pressure due to surface tension is approximately 10 MPa, considering a surface tension γ of 1 N/m^[17]. It should be mentioned that the initial effective pressure of the gas bubble is introduced into the equivalent solid as the initial stresses. It can be seen from Fig.3 that the equivalent solid of the gas bubble exhibits mechanical interaction with the surrounding fuel skeleton even before the application of external pressure, as a result of the mechanical equilibrium that must be maintained. The hydrostatic pressures in the surrounding fuel skeleton are the same as those under the effective pressures applied to the inner surface of the shell model, as obtained with the analytical solutions in Ref. [13]. It is demonstrated that the effects of bubble pressure on the surrounding fuel skeleton can be effectively captured by the stresses in the equivalent solid of FGBs.

While applying external pressure to the spherical model containing FGB, both the volume of the model and that of

FGB decrease. It is known that the bubble pressure should vary with the volume of the FGB in accordance with the modified Van der Waals equation. Fig.4 presents the evolution of bubble pressure with the volume of the FGB, calculated using both FE method and the modified Van der Waals equation. The current volume of the FGB is calculated as $V_0 e^{\epsilon_{kk}}$, and FE results of bubble pressure are calculated as $\frac{1}{3} \sigma_{kk} + \frac{2\gamma}{R_0 e^{\epsilon_{kk}/3}}$. As shown in Fig.4, the evolution of bubble pressure calculated using FE method aligns well with that predicted by the modified Van der Waals equation, thereby verifying the reliability of the established mechanical constitutive equations for the equivalent solid of FGBs.

4 Calculation of Macroscopic Elastic Constants of Irradiated U-10Mo Fuels Using Proposed Mechanical Constitutive Model for Equivalent Solid of FGBs

Macroscale elastic constants (homogenized elastic constants) are key material properties of porous nuclear fuels, directly influencing their mechanical interactions with the cladding in fuel elements. During irradiation, these elastic constants degrade with increasing the macroscopic porosity^[3,13]. The uniaxial tensile test is a standard method for measuring the macroscopic elastic constants of materials^[21]. Therefore, a uniaxial tensile FE simulation based on a representative volume element (RVE) with randomly distributed FGBs in the U-10Mo fuel skeleton is performed, as shown in Fig.5. FGBs are assumed to have identical bubble radii and bubble pressures. To implement the uniaxial tensile test, periodic displacement boundary conditions are applied to the opposite surfaces of RVE to account for its geometric asymmetry. Displacement constraints are applied to nodes 0, 1, 2, and 3 to restrict rigid body movement and rotation of RVE. The uniaxial tensile simulation is performed at a fixed temperature of 373 K, and the number of fission gas atoms is assumed to remain unchanged during the tensile process in this study.

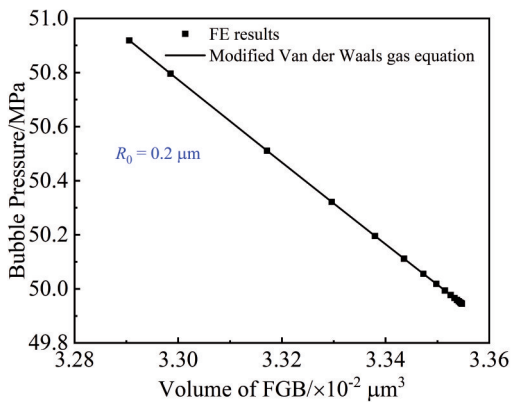


Fig.4 Comparison of bubble pressure evolution results with volume of FGB calculated by FE method and modified Van der Waals equation under external pressure

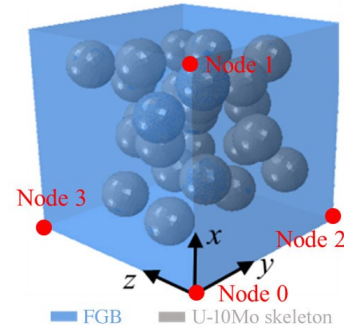


Fig.5 RVE of irradiated U-10Mo fuels with randomly distributed FGBs

According to the homogenization theory, the macroscopic Young's modulus is expressed as follows:

$$\bar{E} = \frac{\bar{\sigma}_x}{\bar{\epsilon}_x} \quad (9)$$

where $\bar{\sigma}_x$ and $\bar{\epsilon}_x$ are the effective stress and strain components in the x direction (the tensile direction), respectively.

The macroscopic Poisson's ratio ($\bar{\mu}$) is calculated as follows:

$$\bar{\mu} = -\frac{1}{2} \left(\frac{\bar{\epsilon}_y}{\bar{\epsilon}_x} + \frac{\bar{\epsilon}_z}{\bar{\epsilon}_x} \right) \quad (10)$$

where $\bar{\epsilon}_y$ and $\bar{\epsilon}_z$ are the effective strain components in the y and z directions, respectively, which are perpendicular to the tensile direction.

The effective stress and strain components are the volume-averaged results of the U-10Mo fuel skeleton and the equivalent solid of FGBs. The effective strain component in the x direction is obtained by Eq.(11):

$$\bar{\epsilon}_x = \frac{\sum_{i=1}^{n_m} \epsilon_{x,i}^m V_i^m + \sum_{j=1}^{n_b} \epsilon_{x,j}^b V_j^b}{\sum_{i=1}^{n_m} V_i^m + \sum_{j=1}^{n_b} V_j^b} \quad (11)$$

where n_m and n_b are the number of the integration points for all the elements of U-10Mo skeleton and the equivalent solid of FGBs, respectively; $\epsilon_{x,i}^m$ and $\epsilon_{x,j}^b$ are the strain components along the x direction for the i -th integration point of the U-10Mo skeleton and the j -th integration point for the equivalent solid of FGBs, respectively; V_i^m and V_j^b are the volume of the i -th integration point for the U-10Mo skeleton and that of the j -th integration point for the equivalent solid of FGBs, respectively. Other effective stress and strain components are calculated similarly.

A representative case with an initial bubble pressure of 50 MPa, a bubble radius of 0.2 μm , and a porosity of 15% for FGBs is selected to analyze the stress field results of irradiated U-10Mo fuels during the uniaxial tensile test. The von Mises stress contour plots on the cross-section in the tensile direction before and after loading are shown in Fig.6. Even in the absence of external loading, a non-uniform distribution of von Mises stress exists within the fuel skeleton, as illustrated in Fig.6a. This uneven stress distribution arises from the effects of the stresses in the equivalent solid of FGBs. Regions with a higher density of FGBs exhibit elevated

von Mises stress due to the interactions between adjacent bubbles. The von Mises stress within the FGBs is zero, as shown in Fig. 6. This indicates that the stress tensors in the equivalent solid of FGBs are spherical ones, representing the effective pressures of FGBs. Upon the application of external loading, the von Mises stress in the U-10Mo fuel skeleton increases continuously, as depicted in Fig. 6b.

The macroscopic Young's modulus is derived from the stress-strain curve of the uniaxial tensile test, based on the slope in the elastic region. Fig. 7 presents the effective stress-strain curve of RVE in the tensile direction during the uniaxial tensile process. It is evident that the effective strain of RVE increases linearly with effective stress. According to Eq. (9), the calculated macroscopic Young's modulus of RVE is about 63 GPa, which is lower than the Young's modulus of dense U-10Mo fuel before irradiation (about 85 GPa). The effective stress component of RVE in the tensile direction starts at zero, as shown in Fig. 7. This indicates that the effective stress component of RVE is zero before the external load is applied,

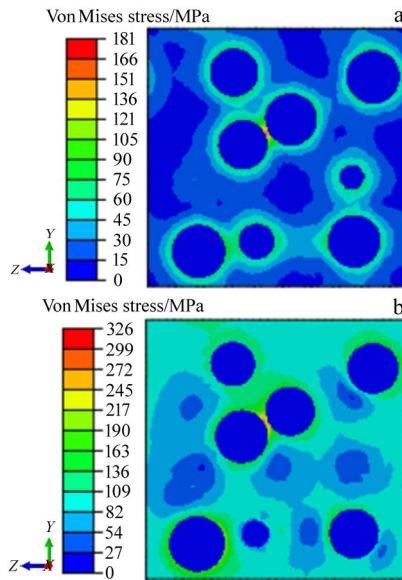


Fig.6 Contour plots of von Mises stress on the cross section in x direction of RVE before loading (a) and after loading (b)

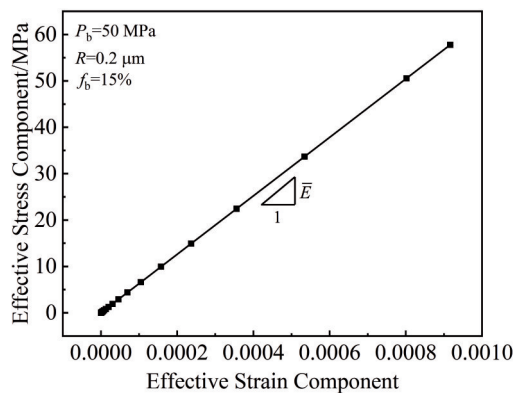


Fig.7 Effective stress-effective strain fitting line of RVE in x direction during loading

despite the non-uniform microscopic stress field within RVE. This suggests that the stress field is self-balanced inside RVE prior to the application of the external load.

Fig. 8 presents the evolution of the effective strain components in the y and z directions relative to the effective strain component in the x direction of RVE. As the effective strain in the x direction increases, the effective strain components in the y and z directions decrease linearly, which is attributed to the Poisson effect. The trends of the effective strain components in the y and z directions are nearly identical. According to Eq. (10), the calculated macroscopic Poisson's ratio of RVE is about 0.316, which is lower than that of the dense U-10Mo fuel before irradiation (about 0.34).

The volume fraction of FGBs inside irradiated U-10Mo fuels increases with irradiation exposure. The bubble pressure and size of FGBs also vary with the local state histories of the irradiated U-10Mo fuels, such as local temperature, hydrostatic pressure, and grain size. According to the study of Li et al^[13], the macroscopic elastic constants of irradiated U-10Mo fuels can be described with the Mori-Tanaka model based on the average volume fraction of intergranular bubbles. However, the effects of bubble pressure and bubble size on the macroscopic elastic constants of irradiated U-10Mo fuels were not discussed in their study due to restrictions in modeling FGBs. In their approach, FGBs were modeled as solids with a small constant elastic modulus, thereby excluding the effects of bubble pressure and surface tension of FGBs. Based on the proposed mechanical constitutive equation for the equivalent solid of FGBs in this study, the macroscopic elastic constants of irradiated U-10Mo fuels with different bubble pressures, sizes, and volume fractions of FGBs are further investigated through simulations of the uniaxial tensile test.

Fig. 9 shows the macroscopic elastic constants of irradiated U-10Mo fuels with varying bubble pressures and volume fractions of FGBs. The bubble pressure ranges from 20 to 120 MPa, while the volume fractions of FGBs vary from 5% to 25%, with a constant bubble radius of 0.2 μm . The macroscopic elastic constants calculated using FE method are compared with those obtained from the Mori-Tanaka model and experimental data^[3]. It can be noted that the macroscopic

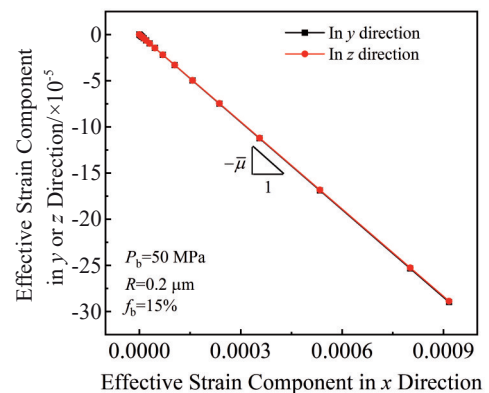


Fig.8 Evolution curve of effective strain in y or z directions versus effective strain in x direction during loading

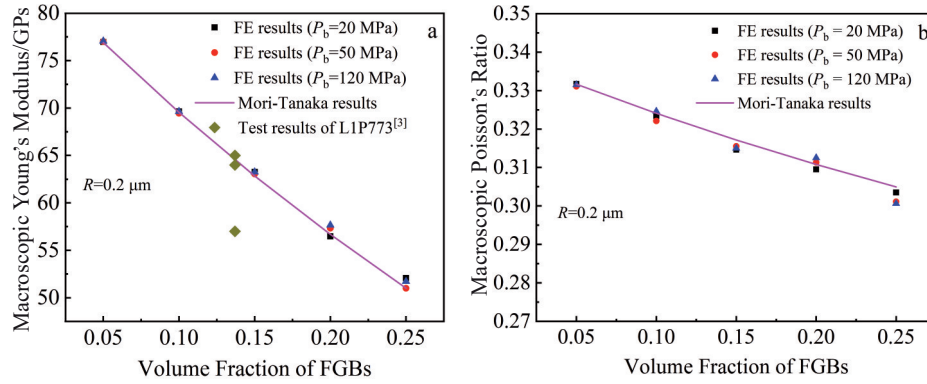


Fig.9 Macroscopic elastic constants of irradiated U-10Mo fuels with different bubble pressure and volume fractions of FGBs: (a) macroscopic Young's modulus; (b) macroscopic Poisson's ratio

elastic constants of irradiated U-10Mo fuels are similar under different bubble pressures, indicating that bubble pressure has a negligible effect on these constants. The results calculated by FE method, based on the proposed mechanical constitutive equation for the equivalent solid of FGBs, are in good agreement with those from the Mori-Tanaka model and experimental data.

Fig.10 shows the macroscopic elastic constants of irradiated U-10Mo fuels with different sizes and volume fractions of FGBs. The uniform bubble radius ranges from 0.1 μm to 1 μm , while the bubble pressure is held constant at 40 MPa. The results indicate that bubble size also has negligible effects on the macroscopic elastic constants of irradiated U-10Mo fuels. The effective elastic constants calculated by FE simulation for fuels with different bubble sizes and volume fractions are consistent with those obtained from the Mori-Tanaka model and experimental data.

5 Discussion

Fig. 11 shows the contour plots of radial stress in the surrounding fuel skeleton before the application of external pressure. It can be seen that the radial stress in the fuel skeleton adjacent to FGB is equal to the hydrostatic stress (negative hydrostatic pressure) of the equivalent solid of FGB. The radial stress in the surrounding fuel skeleton decreases

with increasing distance from FGB. To accurately capture the evolving mechanical interaction between the fuel skeleton and the FGBs under changing irradiation conditions and stress fields, it is essential to establish a mechanical constitutive model for the equivalent solid of FGBs.

According to the homogenization theory, the effective stress components in the x direction of RVE in Fig. 5 can be expressed as $\bar{\sigma}_x = (1 - f_b)\bar{\sigma}_x^m + f_b\bar{\sigma}_x^b$. The components $\bar{\sigma}_x$, $\bar{\sigma}_x^m$, and $\bar{\sigma}_x^b$ correspond to the effective stresses for RVE, the fuel skeleton, and the equivalent solid of FGBs, respectively. Fig. 12 illustrates the evolution results of $\bar{\sigma}_x$, $\bar{\sigma}_x^m$, and $\bar{\sigma}_x^b$ throughout the uniaxial tensile process. FGBs are initialized with a volume fraction of 15%, an average bubble pressure of 50 MPa, and a radius of 0.2 μm . As shown in Fig. 12, before applying the external tensile stress, $\bar{\sigma}_x^m$ is about 7 MPa, whereas $\bar{\sigma}_x^b$ is -40 MPa. The zero value of $\bar{\sigma}_x$ demonstrates that the compressive stress contribution from the equivalent solid of FGBs is balanced by the tensile stress contribution from the fuel skeleton. During the tensile process, both $\bar{\sigma}_x$ and $\bar{\sigma}_x^m$ increase linearly with the effective strain in the tensile direction of RVE, while $\bar{\sigma}_x^b$ remains substantially unchanged. Similar trends in the evolution of $\bar{\sigma}_x$ are observed for the cases with different average pressures and radii of FGBs. This indicates that the U-10Mo fuel skeleton is the primary load-bearing component under

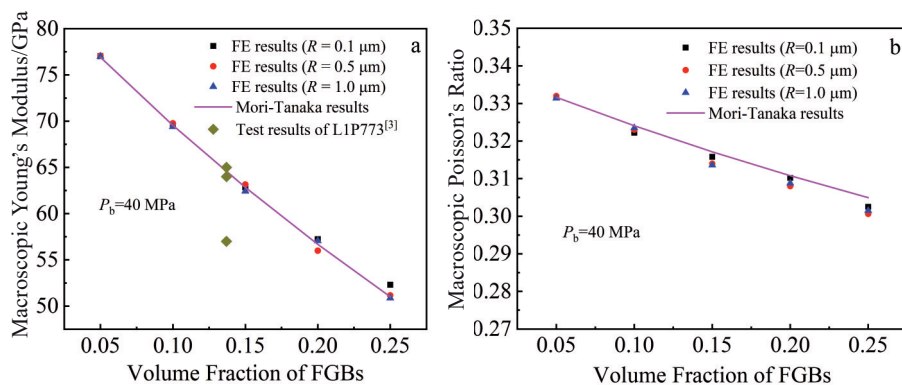


Fig.10 Macroscopic elastic constants of irradiated U-10Mo fuels with different sizes and volume fractions of FGBs: (a) macroscopic Young's modulus; (b) macroscopic Poisson's ratio

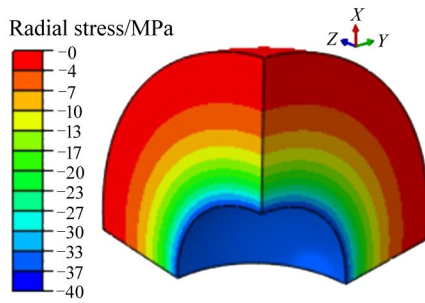


Fig.11 Contour plots of radial stress in surrounding fuel skeleton before application of external pressure

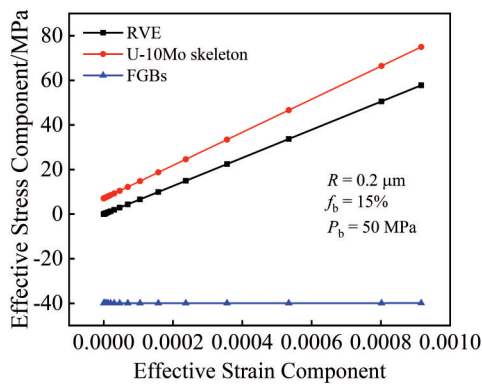


Fig.12 Relationship between effective stress and effective strain in x direction

external tensile stress. The variation in $\bar{\sigma}_x$ is predominantly influenced by $\bar{\sigma}_x^m$ and the macroscopic porosity, rather than the average bubble pressure and radius of FGBs. Thus, it can be concluded that the macroscopic elastic constants of irradiated U-10Mo fuels are primarily determined by the elastic properties of the U-10Mo fuel skeleton and the macroscopic porosity. This finding emphasizes the critical influence of the fuel skeleton on the overall mechanical response of irradiated nuclear fuel.

It is important to note that the volume change of FGBs due to the elastic deformation of the U-10Mo fuel matrix is minimal. The primary mechanisms contributing to the growth of FGBs involve plastic deformation and creep deformation of the fuel skeleton^[5,22], corresponding to the microscale vacancy diffusion and dislocation motion. To account for the time-integration effects of creep deformation during irradiation, the increase in the number of fission gas atoms within FGBs must also be considered. From Eq. (5), it is known that the variations of the number of fission gas atoms^[17,23–24] and temperature can also be taken into account. Consequently, the developed mechanical constitutive model for the equivalent solid of FGBs can also be utilized in thermo-mechanical coupling analyses during prolonged irradiation. This application will offer a more comprehensive understanding of bubble growth behavior and the underlying mechanisms driving this growth.

6 Conclusions

1) The bubble pressure induces non-uniform stress fields in the fuel skeleton, even in the absence of external loading. The maximum von Mises stress is prone to appear in the regions with closely spaced bubbles due to stress interactions between adjacent FGBs.

2) The macroscopic elastic constants of irradiated U-10Mo fuels are found to be minimally affected by bubble pressure and bubble size, which are predominantly determined by the macroscopic porosity. This dependency aligns with the predictions of the Mori-Tanaka model.

References

- 1 Kim Y S, Hofman G L. *Journal of Nuclear Materials*[J], 2011, 419(1): 291
- 2 Burkes D E, Casella A M, Casella A J et al. *Journal of Nuclear Materials*[J], 2015, 464: 331
- 3 Schulthess J L, Lloyd W R, Rabin B et al. *Journal of Nuclear Materials*[J], 2019, 515: 91
- 4 Cao X C, Yang S, Lv J N et al. *Nuclear Engineering and Design*[J], 2023, 412: 112452
- 5 Jian X B, Zhang J, Li Y et al. *International Journal of Plasticity*[J], 2023, 163: 103557
- 6 Finlay M R, Hofman G L, Snelgrove J L. *Journal of Nuclear Materials*[J], 2004, 325(2–3): 118
- 7 Blades A T, Fleming W H, Thode H G. *Canadian Journal of Chemistry*[J], 1956, 34(3): 233
- 8 Petruska J A, Thode H G, Tomlinson R H. *Revue Canadienne de Physique*[J], 1955, 33(11): 693
- 9 Iasir A R M, Peters N J, Hammond K D. *Journal of Nuclear Materials*[J], 2018, 508: 159
- 10 Gan J, Keiser D D, Miller B D et al. *Journal of Nuclear Materials*[J], 2012, 424(1–3): 43
- 11 Casella A M, Burkes D E, Macfarlan P J et al. *Materials Characterization*[J], 2017, 131: 459
- 12 Kim Y S, Hofman G L, Cheon J S. *Journal of Nuclear Materials*[J], 2013, 436(1–3): 14
- 13 Li Y, Ding G C, Xie Z X et al. *Journal of Nuclear Materials*[J], 2023, 579: 154359
- 14 Salvato D, Leenaers A, Van Den B S et al. *Journal of Nuclear Materials*[J], 2018, 510: 472
- 15 Ronchi C. *Journal of Nuclear Materials*[J], 1981, 96(3): 314
- 16 Spino J, Rest J, Goll W et al. *Journal of Nuclear Materials*[J], 2005, 346(2–3): 131
- 17 Cui Y, Ding S R, Chen Z T et al. *Journal of Nuclear Materials*[J], 2015, 457: 157
- 18 Jian X B, Yan F, Kong X Z et al. *Journal of Nuclear Materials*[J], 2022, 565: 153769
- 19 Jiang Y J, Cui Y, Huo Y Z et al. *Nuclear Science and Techniques*[J], 2011, 22(3): 185
- 20 Zhang J, Wang H Y, Wei H Y et al. *Nuclear Engineering and*

- Technology[J], 2021, 53(8): 2616
- 21 Gong Manfeng, Qiao Shengru, Zhang Chengyu et al. *Rare Metal Materials and Engineering*[J], 2009, 38(5): 876 (in Chinese)
- 22 Greenwood G W, Foreman A J E, Rimmer D E. *Journal of Nuclear Materials*[J], 1959, 1(4): 305
- 23 Rest J. *Journal of Nuclear Materials*[J], 2010, 407(1): 55
- 24 Rest J. *Journal of Nuclear Materials*[J], 2010, 402(2-3): 179

辐照后 U-10Mo 燃料裂变气泡的等效固体力学本构模型

李 勇^{1,2}, 严 峰², 张 静², 臧丽叶¹, 丁淑蓉²

(1. 中广核研究院有限公司, 广东 深圳 518026)

(2. 复旦大学 航空航天系 力学与工程仿真研究所, 上海 200433)

摘 要: 辐照后的核燃料裂变气泡存在内压, 导致周围的燃料骨架内部产生应力。为了计算含压裂变气泡所引起的辐照后核燃料的微观力学场, 本研究基于修正的范德华方程, 考虑气泡的表面张力效应, 建立并验证了裂变气泡的等效固体力学本构模型。将裂变气泡等效为固体, 建立了含随机分布裂变气泡的辐照 U-10Mo 燃料的有限元模型, 基于所发展的等效固体力学本构模型、算法及程序, 对辐照后燃料的单轴拉伸试验过程进行了有限元模拟, 获得了微观力学场的分布及演化结果。根据均匀化理论, 获得了辐照 U-10Mo 燃料的宏观弹性常数, 并研究了气泡压力、气泡尺寸和孔隙率对宏观弹性常数的影响。结果表明, 相邻的裂变气泡之间存在力学相互作用, 导致周围骨架产生局部应力集中。辐照后 U-10Mo 燃料的宏观弹性常数随宏观孔隙率的增加而减小, 两者之间的定量关系可以采用 Mori-Tanaka 模型描述。气泡压力和尺寸对宏观弹性常数的影响可以忽略。

关键词: 等效力学本构模型; 裂变气泡; 有限元方法; U-10Mo 核燃料; 宏观弹性常数

作者简介: 李 勇, 男, 1988 年生, 博士, 工程师, 中广核研究院有限公司, 广东 深圳 518026, E-mail: 19110290018@fudan.edu.cn